

Preequilibrium neutron emission in fusion of $^{165}\text{Ho} + ^{12}\text{C}$ at 25 MeV per nucleon

E. Holub,* D. Hilscher, G. Ingold, U. Jahnke, H. Orf, H. Rossner, and W. P. Zank
Hahn-Meitner-Institut für Kernforschung Berlin, 1000 Berlin 39, Federal Republic of Germany

W. U. Schröder

Department of Chemistry and Nuclear Structure Research Laboratory, University of Rochester, Rochester, New York 14627

H. Gemmeke[†]

Fachbereich Physik der Philipps Universität Marburg, 3550 Marburg, Federal Republic of Germany

K. Keller, L. Lassen, and W. Lücking

Physikalisches Institut der Universität Heidelberg, 6900 Heidelberg, Federal Republic of Germany

(Received 1 August 1985)

Neutrons were measured in coincidence with evaporation residues from the reaction $^{165}\text{Ho} + (300 \text{ MeV}) ^{12}\text{C}$. The evaporation residue velocity distribution is indicative of an average transfer of 80% of the full linear momentum in this reaction. The energy spectra of the coincident neutrons exhibit evaporative and preequilibrium components associated with integral multiplicities of $M_{\text{EV}} = (9.5 \pm 0.5)$ and $M_{\text{PE}} = (1.7 \pm 0.3)$, respectively. The experimental neutron energy and angular distributions are analyzed in terms of multiple-source parametrizations, assuming two or three emitters. The results are compared to those obtained from other inclusive and exclusive associated-particle data. It is observed that the emission patterns of the preequilibrium neutrons are in accord with the predictions of a Fermi-jet model, for neutron angles forward of 35° , while this model fails to reproduce the data at angles in the vicinity of 90° and beyond. Various different nucleon momentum distributions have been employed in the model comparison. The insufficiency of the Fermi-jet model to reproduce the data is attributed to the neglect of two-body collisions in this one-body theory. In contrast, the shape of the angle-integrated preequilibrium-neutron energy spectrum is well reproduced with the Harp-Miller-Berne preequilibrium model, if an initial exciton number of $n_0 = 15$ is adopted. This value, as well as the preequilibrium neutron multiplicity, is at variance with systematics established previously.

I. INTRODUCTION

Nonequilibrium light-particle emission is an excellent tool to study the early stages of energy dissipation in heavy-ion-induced reactions. For light-ion-induced reactions, as early as 1954 Gugelot¹ and Eisberg and Igo² observed drastic deviations of experimental particle energy spectra from the predictions of the statistical model for the deexcitation of a fully equilibrated compound nucleus. For instance, Eisberg³ noticed that a statistical interpretation of the 135° spectrum of protons emitted in 31-MeV proton-induced reactions on a heavy target required a thermodynamic temperature of 7 MeV. This would imply that the total excitation energy is confined to only three nucleons, in accordance with the number of initial excitons predicted by the exciton model,⁴ namely a two-particle, one-hole state. This finding led Eisberg to propose a strong competition of compound nucleus with direct processes in energetic light-ion-induced reactions. Very similar ideas have been employed recently to describe light-particle emission in heavy-ion-induced reactions.⁵⁻⁹ It is found in those studies that the high-energy component of the light-particle spectra can be parametrized by assuming isotropic emission of particles with a high-temperature Maxwellian energy spectrum from a source moving in beam direction with about half

the beam velocity. Although this observation allows for a very convenient parametrization of the data, its physical foundation in terms of a hot moving source is still open to debate. The exciton model^{4,10,11} and, similarly, the Harp-Miller-Berne (HMB) model, modified by Blann¹² for heavy-ion reactions, assumes an initial localization of a nonequilibrium ensemble of projectile and target nucleons in phase space that emits light particles with energy spectra very similar to those of a hot moving source model. Furthermore, such spectral shapes are also predicted by Fermi-jet¹³⁻¹⁵ and dissipative diabatic two-center shell models.¹⁶ However, the predicted multiplicity and angular dependence of the emitted high-energy nucleons distinguish the various models.

In order to subject the predictions of these models to crucial experimental tests, it is essential to compare the measured and calculated particle energy spectra at different emission angles. This, however, requires exclusive experiments, since in inclusive experiments the high-energy component of the light-particle spectra is contaminated with particles emitted sequentially from projectile-like fragments, typically at angles forward of 40° . Since these fragments move approximately with beam velocity, the sequentially emitted light particles will be highly energetic in the laboratory system and may, hence, be confused with high-energy particles emitted instantaneously

from the composite system moving with the small center-of-mass velocity. It is possible, however, to avoid contributions of sequential light-particle emission to the experimental spectra by restricting the measurement to light particles emitted in central collisions, in which essentially the whole projectile fuses with the target. Central collisions can be selected experimentally by ascertaining that the detected heavy reaction products carry essentially the full linear momentum.

This can be done either by selecting events according to the correlation angle⁵ of fission fragments, in fusion-fission-like reactions, or by measuring the velocity^{8,9} of fusion-evaporation residues at small angles. Such measurements are very rare at bombarding energies of 10–40 MeV per nucleon above the Coulomb barrier. This range corresponds to energies well above the threshold for pre-equilibrium light-particle emission, placed⁸ at about 5 MeV per nucleon. It encompasses the mean Fermi energy of about 22 MeV of nucleons in nuclei. In the present work, neutron emission in the fusion reaction $^{165}\text{Ho} + ^{12}\text{C}$ at 25 MeV per nucleon bombarding energy, corresponding to 20.5 MeV per nucleon above the Coulomb barrier, is investigated.

In Sec. II below, a brief description of the experimental setup is given. Further details can be found in Refs. 8 and 17. In Sec. III, the data are presented and compared to previous measurements, employing the moving-source parametrization model. In Sec. IV, predictions of the Fermi-jet and the HMB models¹² are compared with the experimental results. In particular, the sensitivity of the experimental data to different Fermi momentum distributions^{18,19} in nuclei is investigated in terms of the Fermi-jet model.

II. EXPERIMENTAL PROCEDURE

The experiments were performed at the VICKSI accelerator of the Hahn-Meitner-Institut, Berlin. Neutrons were measured in coincidence with evaporation residues (ER's) produced in the bombardment of ^{165}Ho with 300-MeV ^{12}C projectiles. The target was a $400\ \mu\text{g}/\text{cm}^2$ thick, rolled metallic holmium foil. The arrangement of ER's and neutron detectors is schematically depicted in Fig. 1. Neutrons were detected with 11 neutron detectors⁸ consisting of 5 or 2.5 cm thick by 12.7 cm diam NE213

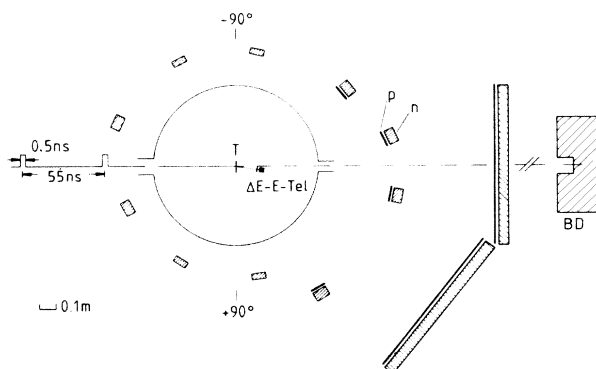


FIG. 1. Schematic diagram of the experimental setup.

scintillators coupled to amperex XP2041 photomultipliers. Ten detectors were arranged in the reaction plane defined by the ER detector, and one detector was placed at 85° out of plane. The flight path varied between 0.68 and 0.98 m. Two 1 m long, 6 cm thick, and 11.5 cm high position-sensitive neutron detectors¹⁷ (also NE213) covered in-plane angles in the range $17^\circ \leq \theta \leq 55^\circ$ ($\phi = 0^\circ$) and $-17^\circ \leq \theta \leq +17^\circ$ ($\phi = 8^\circ$), where ϕ denotes the out-of-plane angle. These detectors were placed at distances from the target of 1.47 and 1.60 m, respectively. The time resolution of the neutron detectors was 1.0 ns FWHM, corresponding to an energy resolution of 20 MeV for 100 MeV neutrons and a flight path of 1 m. For all neutron detectors, n- γ pulse-shape separation techniques^{8,17} were employed. As indicated in Fig. 1, in front of each forward neutron detector and position-sensitive detector a 2 or 4 mm thick plastic scintillator detector, respectively, was used as a veto counter to identify high-energy charged particles.

During the experiment, the energy threshold for neutrons was set at 1 MeV. In the off-line analysis, a neutron energy threshold of 2 MeV was used. In order to determine that the neutron spectra at high energies were independent of the threshold chosen, the analysis was repeated for a neutron threshold of 10 MeV.

Evaporation residues were detected at $\theta_{\text{ER}} = 7.5^\circ$ and 12.3 cm from the target with the $150\ \mu\text{m}$ thick transmission counter of a $\Delta E - E$ solid-state detector telescope with an aperture of 5 mm diam. ER's were easily separated from all other reaction products based on their characteristic time of flight versus energy correlations. The time of flight was measured employing the 0.5–1.0 ns wide cyclotron rf signals for time reference. The separation between two beam bunches was 55 ns. The velocity distribution of all heavy residues detected at 7.5° is shown in Fig. 2. For all neutron coincidences considered below, ER velocities are restricted to $v_{\text{ER}} \geq 0.23\ \text{cm/ns}$, corresponding to velocities larger than $0.5\ v_{\text{c.m.}}$. The center-of-mass velocity $v_{\text{c.m.}}$ corresponding to full linear-momentum

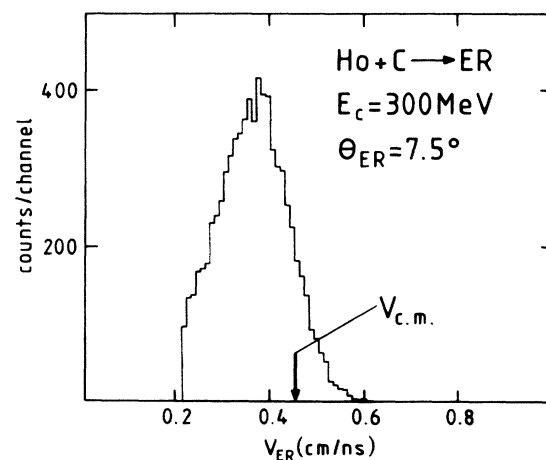


FIG. 2. Velocity distribution of the evaporation residues. No correction for the energy loss in the $400\ \mu\text{g}/\text{cm}^2$ thick target was applied. The arrow indicates the center-of-mass velocity including the mean energy loss in the target.

transfer is 0.47 cm/ns for the Ho + C reaction. The centroid of the velocity distribution at 7.5° shown in Fig. 2 is 0.8 $v_{c.m.}$ after correction for the mean energy loss in the target. However, the absolute values of the measured ER velocities are subject to a systematical error due to the "plasma delay" associated with the detection of heavy fragments,²⁰ which was not taken into account in the analysis. If a plasma delay of 1–2 ns is adopted, the absolute velocities given in Fig. 2 must be reduced by about 3–6%.

All coincidence neutron energy spectra were averaged over neutron detection angles symmetric to the beam direction, in order to average out distortions of the spectra introduced by the recoil imposed to the ER's by the detected neutrons.^{8,21}

III. EXPERIMENTAL RESULTS

Double-differential multiplicities of neutrons in coincidence with evaporation residues are shown in Fig. 3. These spectra obviously consist of two components. A low-energy component is consistent with neutron evaporation from a thermally equilibrated compound nucleus.

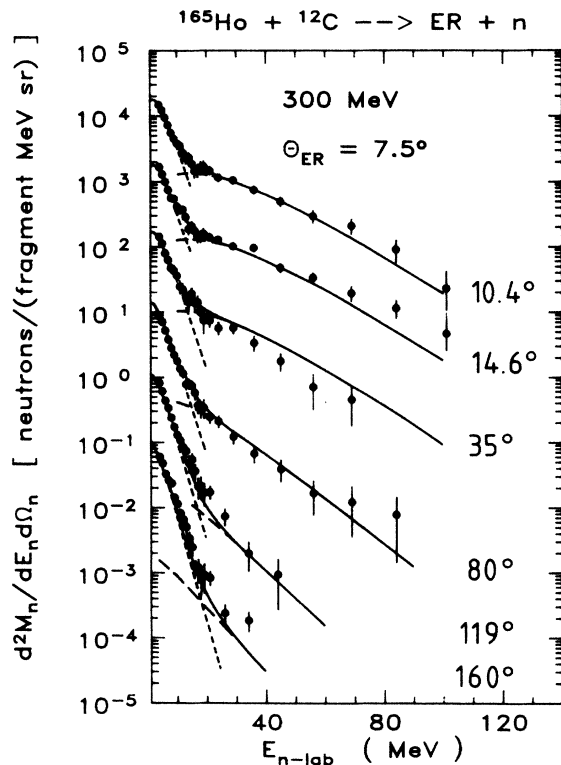


FIG. 3. Experimental differential neutron multiplicities (data points) in coincidence with evaporation residues detected at 7.5° having velocities larger than 0.23 cm/ns (see Fig. 2). The short- and long-dashed curves are the results of the least-square fits to evaporative and preequilibrium components, respectively. The solid curves represent the sums of both components. The parameters of the curves are given in Table I. The spectra at 10.4°, 14.6°, 35°, 80°, 119°, and 160° were multiplied by 10ⁿ, with n being 5, 4, 3, 2, 1, and 0, respectively.

The high-energy component is attributed to preequilibrium neutron emission occurring before a thermal equilibrium has been attained by the composite system. The multiplicity of neutrons with laboratory energies above 100 MeV, corresponding to twice the beam velocity, is found to be $(3 \pm 1) \times 10^{-3}$. This implies that the probability for transferring more than 35% of the available relative kinetic energy to a single neutron is 3×10^{-3} .

Both neutron energy components show an exponential slope, making it very convenient to parametrize these spectra in terms of Maxwellians, i.e.,

$$dM_n/dE_n \propto \sqrt{E_n} \exp(-E_n/T).$$

Assuming isotropic statistical emission from a moving source, the energy-differential angular distribution of the neutron multiplicity is given by²²

$$\frac{d^2M_n}{dE_n d\Omega_n} = \frac{M_n}{2(\pi T)^{3/2}} \sqrt{E_n} \times \exp[-(E_n - 2\sqrt{\epsilon E_n} \cos\theta_n + \epsilon)/T]. \quad (1)$$

Here, the quantities M_n , T , and ϵ correspond to the multiplicity, temperature parameter, and energy per nucleon of the moving source, respectively. For the evaporative component, a source velocity in beam direction with magnitude equal to the c.m. velocity $v_{c.m.}$ is adopted. A least-square fit of a superposition of two theoretical distributions of the form of Eq. (1) to the experimental data was performed using M_{EV} , T_{EV} and M_{PE} , T_{PE} , and ϵ_{PE} as free parameters. The subscripts EV and PE refer to evaporation and preequilibrium emission, respectively. In Fig. 3, the best fits of the EV and PE component are shown by short- and long-dashed curves, respectively, while the solid curves represent the theoretical sum spectra. The parameters of the best fit are collected in Table I. The multiplicity values quoted are based on an extrapolation of the neutron yield to energies below the experimental threshold, employing the functional form of Eq. (1). As can be seen from Fig. 3, it is possible to adequately parametrize the data using the stated assumptions about two emitters.

The same methods of parametrization have been used for most of the inclusive and exclusive data reported in the literature as for the data examined here, so it is possible to compare the results for the parameters deduced for the different reactions studied. The source velocity obtained in the present experiment for the PE component, using the fitting procedure described above, is (0.5 ± 0.14) times the beam velocity. This finding is similar to observations made^{5–8} in all previous experiments. It is not

TABLE I. Parameters of a least-square fit using Eq. (1) and two moving sources.

	M	T (MeV)	ϵ (MeV/nucleon)
EV	9.5 ± 0.5	2.75 ± 0.2	0.115^a
PE	1.7 ± 0.3	10.7 ± 1.0	5.7 ± 0.5

^aEnergy per nucleon of the center of mass.

possible, however, to compare the multiplicity of particles measured in exclusive experiments with inclusive data, since in the latter case the impact parameters or the reaction cross section contributing to the light-particle emission are not known. For the exclusive measurement of proton emission in central $^{238}\text{U} + ^{16}\text{O}$ collisions at 14 MeV per nucleon above the barrier, Awes *et al.*⁵ quote a proton multiplicity of 0.47, compared to an estimated proton multiplicity of 1.45 for the present reaction at 20.5 MeV per nucleon above the barrier. The latter multiplicity is obtained from the experimental parameters for pre-equilibrium neutron emission given in Table I, corrected for a proton emission threshold of 6 MeV due to the Coulomb barrier. The larger multiplicity observed in the present experiment can be attributed to the higher bombarding energy.

The temperature parameters deduced from the present high-energy neutron spectra are compared in Fig. 4 with the results of previous measurements. One observes that the temperature parameters for neutron-ER coincidences are clearly larger than those inferred^{6,7} from inclusive proton data. The following observation provides a possible explanation for this discrepancy. The neutron-ER coincidence measurement selects central collisions with linear-momentum transfers that are larger than the average values associated with inclusive measurements and, hence, it samples "hotter" sources. The inclusive data, on the other hand, average over a larger range of impact parameters. The effect of the ER velocity on the neutron energy spectra has been demonstrated by Hilscher *et al.*²³ This interpretation is supported by the exclusive proton data of Awes *et al.*⁵ (open circle in Fig. 4), measured in coincidence with fission fragments, with the magnitude of the linear-momentum transfer being determined from the correlation angle of the two fission fragments.

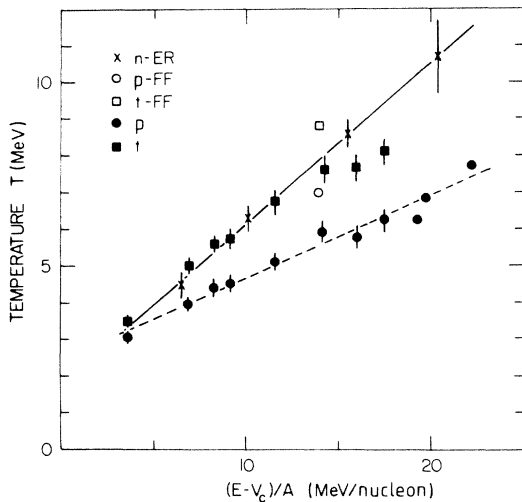


FIG. 4. Temperature parameters T_{PE} versus energy per nucleon above the barrier; (\times) corresponds to neutrons measured in coincidence with ER (Ref. 8) and the present result (Table I), open and filled circles (squares) correspond to exclusive (Ref. 5) and inclusive (Refs. 6 and 7) proton (triton) data, respectively. The solid and dashed lines are drawn through the exclusive n and inclusive p data, respectively.

In Fig. 4, the PE-temperature parameters obtained from inclusive triton data are included as solid squares. It is, at first, surprising to observe that the magnitudes of the triton temperature parameters T_{PE}^t are consistent with the exclusive neutron data but exceed the values reported for inclusive proton experiments by about 30%. One should note, however, that the values of the temperature parameters deduced from fits of experimental particle energy spectra depend on the shape of the theoretical energy spectrum adopted in such fits. All light-particle spectra discussed here have been fitted with a Maxwellian shape, i.e., $d\sigma/dE \propto E^{1/2} \exp(-E/T_M)$, in order to deduce the temperature parameter T_M . While such a parametrization appears appropriate for a description of nucleons emitted in an evaporation chain, the actual shape of pre-equilibrium energy spectra of composite particles is not well known. Consequently, a systematic uncertainty has to be attributed to the temperature parameters deduced from the slopes of experimental energy spectra. To demonstrate this model dependence, one can adopt the coalescence model²⁴ which predicts for the energy spectrum of a composite particle containing A nucleons the simple power law

$$\frac{d\sigma(E)}{dE} \propto \left[\left(\frac{E}{A} \right)^{1/2} \exp \left(-\frac{E}{AT_A} \right) \right]^A \propto E^{A/2} \exp \left[-\frac{E}{T_A} \right]. \quad (2)$$

Here, the quantity T_A corresponds to the temperature parameter associated with the emission of individual nucleons. For an equivalent reproduction of experimental spectra with a Maxwellian or Eq. (2), the respective temperature parameters obey the relation

$$T_A = T_M \left[1 + \frac{(A-1) T_M}{2 E} \right]^{-1}. \quad (3)$$

Evaluating Eq. (3) for tritons with an average energy of $\langle E \rangle \approx 5T_M$ representative of the range used in the fits, one obtains $T_{A=3} \approx 0.8T_M$. These values are now in reasonable agreement with the temperature parameters deduced from inclusive proton data, resolving an apparent discrepancy in the data displayed in Fig. 4. However, this observation should not be construed as an endorsement of the coalescence model, but should merely demonstrate the latitude available in the interpretation of experimental data.

In addition, it is important to note that the parameters mentioned above are obtained under the assumption that only two sources contribute significantly to pre-equilibrium neutron emission in the $^{165}\text{Ho} + ^{12}\text{C}$ reaction. The justification for this assumption is derived from the fact that the measured light-particle spectra show only one low- and one high-energy component. However, it is conceivable that the high-energy component might be due to neutron emission from two independent sources moving

with different velocities. In order to test this assumption, a least-square fit of the present data using three sources instead of two was also performed. The spectral shapes are the same as given in Eq. (1). The results are given in Table II. The parameters of the evaporative part have not changed from the results of the previous analysis, but the value of the chi-squared per point of the fit to the high-energy component above 20 MeV has improved by a factor of 2 compared to the two-source fit. This is not surprising, since the number of parameters has increased by a factor of 2 as well. It is interesting to observe, however, that the fit suggests the presence of a fast source (PE2), moving with almost beam velocity, in addition to a slow source (PE1), moving only somewhat faster than the center of mass. The temperature parameters are about the same for both of these sources and close to those obtained in the two-source fit. In Table II, instead of errors of the parameters deduced in the fit assuming two preequilibrium sources (PE1 and PE2), a second set of parameters consistent with the data is indicated in parentheses, associated with a somewhat larger chi-squared per point. This demonstrates a relatively large ambiguity of the data with respect to different parameter sets. Although the three-source fits lead to ambiguous parameter sets, they always provide one fast- and one slow-moving source with a high temperature parameter matching that obtained in the two-source fit.

Taking the three-source parametrization to have a physical foundation leads to the implication either (i) that peripheral interactions are contributing to ER production, (ii) that nucleons are also being emitted in the approach phase, or (iii) that in a central collision, a fast-moving source (PE2) that can be simulated by a Fermi-jet mechanism coexists with a slow-moving source (PE1) due to two-body collisions. Interpretation (iii) agrees with the theoretical predictions by Cassing.²⁵ To summarize the results of the multiple-source fits to the PE component, no unique parametrization is obtained; the parameter sets deduced from these fits are useful only as summaries of the experimental data, but do not provide an obvious image of the underlying physical processes.

Since the mean linear momentum transfer to the evaporation residues can be deduced from the measured mean velocity of the ER, it is possible to determine the extent to which preequilibrium light-particle emission accounts for the missing momentum and excitation energy of the compound nucleus. The mean linear momentum transfer is found to be 80% of its maximum value. In order to calculate the missing excitation energy, it is assumed that the

fraction of missing linear momentum corresponds to the fraction of nucleons from the projectile which do not participate in the fusion process but rather undergo a single scattering from a target nucleon. This picture predicts the emission of twice as many free nucleons from an apparent source moving with half the beam velocity. The missing energy is calculated to be 84 MeV, while the maximum total excitation energy of the completely fused system amounts to 267 MeV. This would result in a mean temperature of the evaporated neutrons of about 2.65 MeV and a neutron multiplicity of 10.3, as calculated with the evaporation code JULIAN. In order to estimate the nuclear temperature, a level density parameter of $a = A/8$ is used. In comparison, from the two-source fit, a temperature of (2.75 ± 0.2) MeV and a neutron multiplicity of $M_{EV} = (9.5 \pm 0.5)$ is obtained, in approximate agreement with the above estimate. The parameters obtained from the preequilibrium source fits can be used to calculate that an excitation energy of

$$E \approx M_{PE}(B_n + 1.5T_{PE} + \epsilon_{PE}) = 49 \text{ MeV}$$

is carried away by the high-energy neutrons. Here, B_n is the neutron binding energy. Therefore, the neutrons emitted prior to attainment of thermal equilibrium already account for more than half of the missing excitation energy. Similarly, about one-third of the missing momentum is carried away by such neutrons. Hence, major fractions of missing momentum and excitation energy can be attributed to preequilibrium light-particle emission, assuming that protons not measured in the present experiment have multiplicities and energy spectra similar to those of the measured neutrons.

IV. COMPARISON WITH THEORETICAL MODELS

A. Fermi-jet model

The basic idea of the Fermi-jet or PEP (promptly emitted particle) model¹³ is that nucleons can be exchanged through a window between approaching reaction partners, pictured as containers of two interacting Fermi gases. The addition of the velocity of relative motion of the two nuclei and the Fermi velocity of nucleons can result in highly energetic nucleons in the recipient nucleus that have a finite chance to escape directly, without further interaction. This model has been previously compared with heavy-ion-induced precompound nucleon emission.^{8,13,15,26} Some of these comparisons⁸ showed that this model¹³ cannot explain the yields of high-energy neutrons near 90°. Leray *et al.*¹⁵ have used essentially the same model, but account for Pauli blocking as well as for the velocity and the spatial extension of the window between the two interacting nuclei. According to Leray *et al.*,¹⁵ especially the latter treatment of the window geometry results in enhanced yields of high-energy neutrons from central Ho + Ne collisions⁸ at 11, 15, and 20 MeV per nucleon, in the angular range of 60°–90°.

It was pointed out by Schröder and Huizenga²⁷ that an incorrect modeling of the Fermi-velocity distribution could be partially responsible for the insufficiency of the model of Bondorf *et al.*¹³ to reproduce the yields of

TABLE II. Parameters of a least-square fit using Eq. (1) and three moving sources. A second set of parameters consistent with the data is given in parentheses.

	M	T (MeV)	ϵ (MeV/nucleon)
EV	9.5 ± 0.5	2.75 ± 0.2	0.115^a
PE1	$1.6(0.6)$	$9.0(9.2)$	$1.7(0.13)$
PE2	$0.3(1.1)$	$7.6(9.9)$	$22.6(9.9)$

^aEnergy per nucleon of the center of mass.

high-energy neutrons emitted at large angles. In the present work, several different Fermi momentum distributions are employed with the Fermi-jet model. They include those proposed by Lifshitz and Singer,¹⁹ who showed that rather broad distributions in nucleon momenta p are necessary to describe measured neutron energy spectra following μ capture in nuclei. The following three hypothetical distributions are considered in the present analysis:

(i) a finite-temperature Fermi distribution:

$$\frac{dW}{dv^3} = \left\{ 1 + \exp \left[\left(\frac{m}{2} v^2 - \mu \right) / T \right] \right\}^{-1}$$

where

$$\mu = \epsilon_F \left[1 - \frac{\pi^2}{12} \left(\frac{T}{\epsilon_F} \right)^2 \right];$$

(ii) a Gaussian distribution:¹⁹

$$dW/dp^3 = \exp(-p^2/\alpha^2)$$

with

$$\alpha^2/2m_0 = 20 \text{ MeV};$$

(iii) the Amado-Woloshyn distribution:¹⁸

$$dW/dp^3 = N \cosh^{-2}(\gamma p)$$

where¹⁹

$$\gamma = 0.8 \text{ fm}/\hbar.$$

The momentum distributions (ii) and (iii) were converted to velocity (v) distributions by setting $v = p/m_0$ where m_0 is the free-nucleon mass. The calculated double-differential neutron multiplicities are shown in Fig. 5 for a Gaussian (ii) or Amado-Woloshyn (iii) distribution. As can be inferred from this figure, the yields of high-energy neutrons are significantly overestimated by both models at almost all angles. Even the slopes of the theoretical energy spectra do not agree with the experimental ones. This discrepancy may either indicate that it is incorrect to transform the momentum distribution into velocity distributions by letting $v = p/m_0$, or signify an inapplicability of such momentum distributions in the process considered. The large momentum components in these distributions do not necessarily correspond to large velocity components of nucleons moving freely within the mean field. Rather they are due to few-nucleon correlations, such that these momentum distributions could be realistic only for a modeling of the two-body collisions of nucleons inside the two interacting Fermi spheres that can lead to PEP emission. The large momentum components will then, of course, result in high-energy nucleons at large angles. In fact, distribution (iii) was originally proposed by Amado and Woloshyn,¹⁸ in order to describe the two-body backward scattering of 600–800-MeV protons.

Only the finite-temperature Fermi distribution results in a reasonable agreement (Fig. 6) with the data at forward and backward angles if a temperature of about 6 MeV is used. However, it is not possible to reproduce the yield near 90° in this model. This is probably due to the

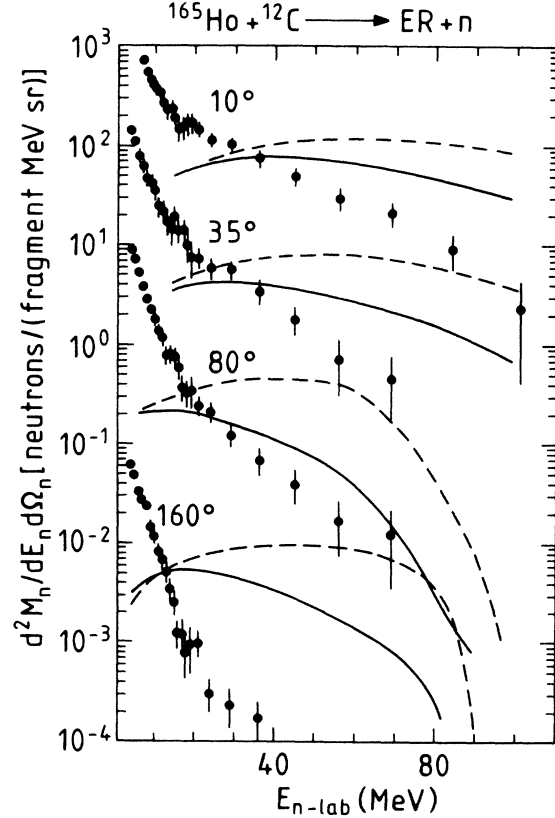


FIG. 5. Comparison of the experimental double-differential neutron multiplicity and the Fermi-jet model using a Gaussian (Ref. 19) (solid curves) or an Amado-Woloshyn (Ref. 18) (dashed curves) velocity distribution, at 10°, 35°, 80°, and 160°. Data and calculations were multiplied by factors of 10^4 , 10^3 , 10^2 , and 1, respectively.

omission of the rescattering of nucleons inside the interacting Fermi spheres, which is treated only incompletely by taking into account the absorption of nucleons. The contribution of high-energy nucleons at forward and backward angles can, hence, be understood in terms of direct Fermi jet emission, provided the finite-temperature Fermi distribution represents a realistic model for the high-momentum components of nucleons in nuclei. However, at angles near 90° and beyond, two-body collisions are expected to compete strongly with one-body Fermi-jet emission, as shown by Cassing.²⁵ If rescattering effects are to be taken into account quantitatively, it may prove necessary to consider more realistic Fermi momentum distributions in nuclei than assumed in the present analysis.

B. Comparison with the modified Harp-Miller-Berne model

The application of exciton-type approaches^{6,8,11,12,28–32} to preequilibrium emission of light particles in heavy-ion-induced reactions has already shown considerable success. One can distinguish mainly two models: the exciton model^{4,10} as used by Machner,¹¹ and the Harp-Miller-Berne model modified by Blann¹² for application to heavy-ion-induced reactions. Both of these models treat the evolution of preequilibrium cascades towards equi-

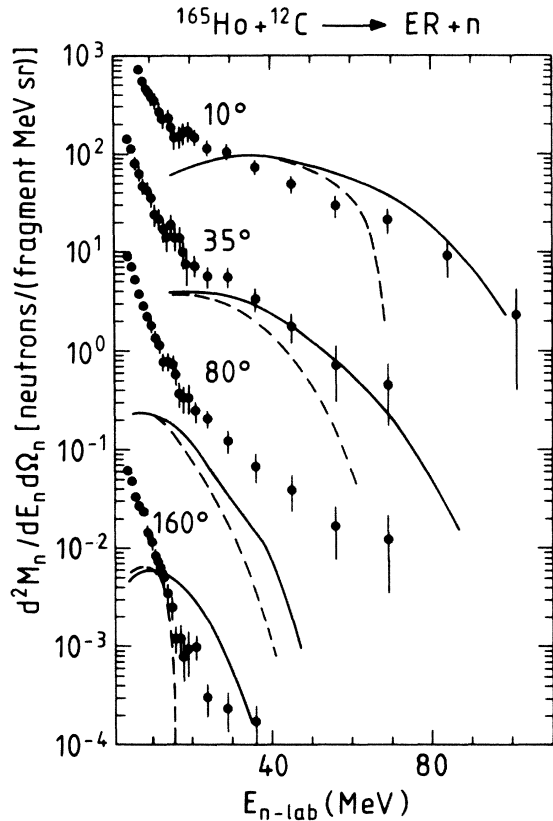


FIG. 6. Same as Fig. 5. The solid and dashed lines are the results of the Fermi-jet calculation using the finite-temperature Fermi momentum distributions (i) for $T=6$ and 0 MeV, respectively.

brium in terms of a Boltzmann master equation approach.

In the Harp-Miller-Berne model, the equilibration of the target-projectile system is considered in terms of a time-dependent single-particle occupation probability distribution of small bins in total available excitation energy. The relaxation of the system is achieved either by internal nucleon-nucleon scattering, or by particle emission into the continuum. The shape of the emitted particle spectrum is mainly determined by the initial degree of freedom, the initial exciton number n_0 .

Within the exciton model the equilibration of the system is described as the time dependent evolution of a chain of successive particle-hole excitations. The master equation for the occupation probability of a state with a given number of particles and holes (together, excitons) governs the equilibration of the system. From each exciton state the system can deexcite either by two-body scattering into more or less complex exciton states or by emission into the continuum. The shape of the emitted particle spectra is also mostly determined by the initial exciton number n_0 . The meaning of this parameter in the exciton model is more plausible, being simply the initial particle-plus-hole number. The exciton model¹¹ is able to predict angular distributions of the emitted particles, while within the modified HMB model^{12,29} only angle-integrated spectra are calculated.

The present experimental neutron spectra are compared below to the predictions of the modified HMB model.¹² Using the parameters obtained by fitting the double-differential neutron spectra with a Maxwellian shape (Table I), the angle-integrated spectrum corresponding only to the preequilibrium component is calculated. From the modified HMB calculation, several parameters can be determined. The most significant one is the initial degree of freedom or exciton number n_0 , which determines the slope of the spectrum. From Fig. 7, one observes that for $n_0=15$ and an intensity scaling parameter of $K=1$, the shape of the calculated neutron spectrum is in agreement with the data. However, in order to obtain the correct magnitude of the multiplicity, an additional intensity scaling ($K>1$) of the calculated spectra is necessary, since with a scaling factor of $K=1$ (and $n_0=15$), the calculated spectrum underestimates the data by about a factor of 2. The scaling can be done, for instance, by reducing the exciton transition rates, i.e., by increasing the nucleon mean free path length. This increases the time that the system spends in a given configuration and, hence, the number of emitted particles increases. Consequently, the equilibration times also increase. For the case with $K=1$, the preequilibrium component has developed fully already after 10 unit time steps of $\Delta t=2.1 \times 10^{-23}$ s. However, in order to obtain a good quantitative reproduction of the data, $K=4$ and 20 unit time steps are needed with $n_0=15$. Such a correlation between transition rates and equilibration periods arises naturally. It is emphasized that using $K=1$ and $n_0=12$ with the modified HMB model²⁹ results in only a very rough description of the data. The above comparison of data and calculations, hence, provides a value of the model parameter n_0 determining the shape of the energy spectra that is larger than the number of nucleons in the projectile, as also noticed in

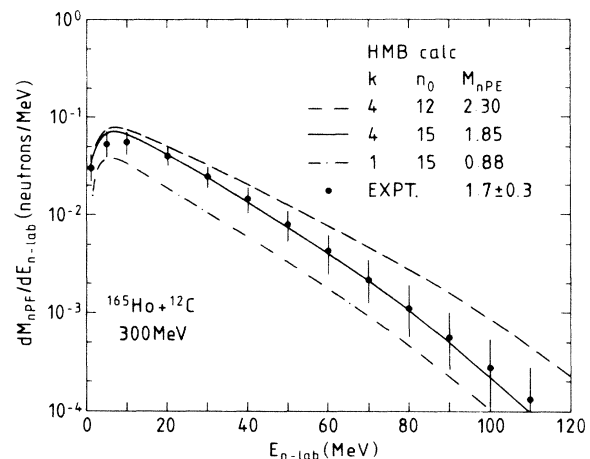


FIG. 7. Comparison of the HMB-model calculation for different initial exciton numbers (n_0) and transition-rate scaling factors (K) with experimental preequilibrium energy spectra of $^{165}\text{Ho} + ^{12}\text{C} \rightarrow \text{Er} + n$. The experimental angle-integrated energy spectrum was obtained by integrating Eq. (1) over angle and using the PE parameters given in Table I. The error bars shown correspond to the uncertainties of the parameters M_{PE} , T_{PE} , and ϵ_{PE} given in Table I.

other experimental analyses.^{8,21} However, the implications of the need for the additional scaling of the model calculation for the validity of the basic relaxation process in heavy-ion-induced reactions assumed in the model are as yet not clear. A similar reduction by a factor of 4 of the transition rates has been used by Machner^{11,32,33} in the extended exciton model.

In order to derive an independent estimate (n_0^{GR}) for the initial degree of freedom, n_0 , it is also possible to inspect the Griffin plot³⁰ (GR) of the present data. Recently, this method has been applied in several studies^{8,28,31} of preequilibrium emission of light particles in heavy-ion-induced reactions. The Griffin plot of the present data for the very high energies ($E_{\text{n lab}} > 60$ MeV) suggests $n_0^{\text{GR}} = 16$, a value close to the estimate ($n_0^{\text{HMB}} = 15$) obtained using the HMB model calculation.

The present data give valuable information also about the bombarding-energy dependence of the initial exciton number n_0 in heavy-ion reactions.^{28,31,32} Figure 8 exhibits systematics³¹ of the dependence of the quantity $\Delta n_0^{\text{HMB}} = n_0^{\text{HMB}} - A_p$ (A_p is the projectile mass) on $(E_{\text{c.m.}} - V_c)/\mu$, in the range of energies from 5–20 MeV per nucleon. In the figure only coincidence data are included. The data are not conclusive. They show partly an indication of an increase of n_0 with energy, but not for all data sets consistently. The strongest increase is observed for neutron spectra in coincidence with fusion-fission fragments from $^{165}\text{Ho} + ^{20}\text{Ne}$ at energies between 220 and 402 MeV; n_0^{HMB} varies⁸ from 20 to 28. The neutron-ER data for the same reaction indicate only a slight increase with energy; n_0^{HMB} varies from 20 to 23, in the above energy range. The present data show that, for the reaction $^{165}\text{Ho} + ^{12}\text{C} \rightarrow \text{ER} + \text{n}$ at the high bombarding energy of 20.6 MeV per nucleon above the Coulomb barrier, the initial exciton number n_0 increases only by 3 to 4 units from the projectile mass number. All presented data seem to indicate that $n_0^{\text{HMB}} - A_p$ remains approximately constant at higher energies above the barrier. To understand more precisely the n_0 behavior for various reactions and energies, further data are needed.

Somewhat different results are systematically obtained by applying the extended exciton model to heavy-ion-

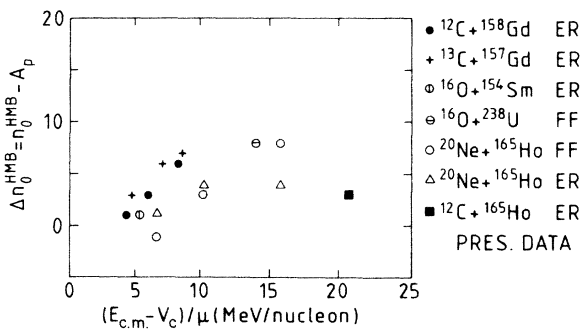


FIG. 8. Extracted exciton number excess over the projectile mass number, $n_0^{\text{HMB}} - A_p$, versus center-of-mass energy per nucleon above the Coulomb barrier for different systems taken from Ref. 31 for exclusive data only. The square is the present result.

induced preequilibrium emission.^{11,32} For $^{165}\text{Ho} + ^{20}\text{Ne} \rightarrow \text{ER} + \text{n}$ at energies of 220, 292, and 402 MeV,⁸ the exciton model calculation (EM) (Ref. 11) gives $n_0^{\text{EM}} = 22$ particles (p) + 2 holes (h), $25p + 5h$, and $30p + 10h$, respectively. The same model applied to the present $^{165}\text{Ho} + ^{12}\text{C}$ data predicts³² $n_0^{\text{EM}} = 15p + 3h = 18$ excitons. All analyses suggest somewhat larger exciton numbers n_0^{EM} , as compared to n_0^{HMB} or (sometimes) n_0^{GR} . The significance of this observation of a definite model dependence of the initial exciton number n_0 is presently uncertain.

V. CONCLUSION

Central collisions of ^{165}Ho and ^{12}C at 300 MeV are observed to result in compound nuclei carrying, on the average, approximately 80% of the full linear momentum in the reaction. It is found that 85% of all emitted neutrons are evaporated from a thermally equilibrated system, whereas 15% are emitted prior to the attainment of such an equilibrium. The double-differential neutron multiplicities can be parametrized with multiple-source fits using two or three emitting sources. With a two-source fit, one identifies a slow-moving evaporating source and a fast source moving with half the beam velocity and emitting neutrons with a hard energy spectrum corresponding to a high temperature parameter. Assuming three sources to be present in a collision, the parameters describing the evaporative source are found to be unchanged, whereas the high-energy neutron component is best represented by a superposition of spectra of neutrons emitted from either a fast- or a slow-moving source with about the same temperature parameters. Although the parameters derived from three-sources fits to particle angle and energy distributions are not well defined, the present analysis suggests that it may not be justified to draw definite conclusions about the physical meaning of parameters obtained in such multiple-source fits. In particular, the existence of a preequilibrium particle emitter, moving with half the beam velocity, as suggested by two-sources representations of the present data, is not conclusive, since the same data can be explained by the coexistence of a slow- and a fast-moving source. Hence, it remains for future studies to clarify whether or not a spatially localized, "hot moving source" of A nucleons of the projectile and a similar number of target nucleons is produced in energetic collisions between heavy ions.

If one nevertheless adopts the validity of the physical picture of a two-sources model, one finds that almost half of the energy and linear momentum missing from the compound nucleus produced in a central collision can be accounted for in terms of preequilibrium neutron emission. Furthermore, a comparison of the temperature parameters obtained in this work with those reported previously for inclusive and exclusive measurements of nucleon emission indicates that, for energies below 25 MeV per nucleon, temperature parameters are larger for exclusive than for inclusive data. It is suggested that this behavior is due to the rather different impact parameter ranges contributing to inclusive and exclusive data. Whereas more peripheral collisions with smaller temperatures are probed in inclusive experiments, more central collisions

are selected in coincidence experiments. An apparent disparity between temperature parameters deduced from inclusive triton and proton data could possibly be attributed to different functional forms of the energy spectra of nucleons and composite particles, as, for example, suggested by the coalescence model. However, other model explanations cannot be ruled out on the basis of the experimental particle energy spectra.

The experimental neutron energy spectra obtained in this work are compared with the Fermi-jet and Harp-Miller-Berne models. Adopting a particular form of the momentum distribution, the Fermi-jet model, neglecting two-body collisions, can reproduce the measured energy spectra, but only at angles smaller than 35° . Employing different Fermi-velocity distributions does not provide a better agreement between theory and experiment at small angles, as well as at angles around 90° . Following a suggestion by Cassing,²⁵ it is argued that the high-energy neutron yield around 90° is mainly due to two-body collisions.

A comparison with the HMB model indicates that the measured spectral shape can be described best with an initial exciton number of only $n_0=15$. This is at variance with recently reported^{28,31,32} systematics on the variation of the exciton number with bombarding energy that predicts an exciton number of about 20–30 for the $^{165}\text{Ho} + ^{12}\text{C}$ reaction. In addition, in order to also reproduce the absolute magnitude of the preequilibrium neutron multiplicity, it is necessary to increase the exciton transition rates employed in the model by a factor of 4, as compared to the nominal values suggested by Blann.²⁹

ACKNOWLEDGMENTS

This work was partially supported by the U.S. Department of Energy and by the Bundesministerium für Forschung und Technologie. The financial support of one of the authors (E.H.) by the International Bureau for Scientific Collaboration in Jülich (KFA) is gratefully appreciated. We would also like to thank W. Cassing and H. Machner for many stimulating discussions.

*On leave from the Rudjer Bošković Institute, Zagreb, Yugoslavia. Present address: Fritz-Haber-Institut, 1000 Berlin-33, Federal Republic of Germany.

†Present address: Institut für Kernphysik I, Kernforschungszentrum Karlsruhe, 7500 Karlsruhe, Federal Republic of Germany.

¹P. C. Gugelot, Phys. Rev. **93**, 425 (1954).

²R. M. Eisberg and G. Igo, Phys. Rev. **93**, 1039 (1954).

³R. M. Eisberg, Phys. Rev. **94**, 739 (1954).

⁴J. J. Griffin, Phys. Lett. **24B**, 5 (1967); M. Blann, Annu. Rev. Nucl. Sci. **25**, 123 (1975).

⁵T. C. Awes, G. Poggi, C. K. Gelbke, B. B. Back, B. G. Glagola, H. Breuer, and V. E. Viola, Jr., Phys. Rev. C **24**, 89 (1981).

⁶T. C. Awes, S. Saini, G. Poggi, C. K. Gelbke, D. Cha, R. Legrain, and G. D. Westfall, Phys. Rev. C **25**, 2361 (1982).

⁷R. Glasow, G. Gaul, B. Ludewigt, R. Santo, H. Ho, W. Kühn, U. Lynen, and W. F. J. Müller, Phys. Lett. **120B**, 71 (1983).

⁸E. Holub, D. Hilscher, G. Ingold, U. Jahnke, H. Orf, and H. Rossner, Phys. Rev. C **28**, 252 (1983).

⁹A. Gavron, J. R. Beene, R. L. Ferguson, F. E. Obenshain, F. Plasil, G. R. Young, G. A. Petit, K. Geoffroy Young, M. Jääskeläinen, D. G. Sarantites, and C. F. Maguire, Phys. Rev. C **24**, 2048 (1981); A. Gavron, J. R. Beene, B. Cheynis, R. L. Ferguson, F. E. Obenshain, F. Plasil, G. R. Young, G. A. Pettitt, C. F. Maguire, D. G. Sarantites, M. Jääskeläinen, and K. Geoffroy-Young, *ibid.* **27**, 450 (1983).

¹⁰G. Mantzouranis, H. A. Weidenmüller, and D. Agassi, Z. Phys. A **276**, 145 (1976).

¹¹H. Machner, Phys. Rev. C **28**, 2173 (1983).

¹²M. Blann, Phys. Rev. C **23**, 205 (1981).

¹³J. P. Bondorf, J. N. De, G. Fai, A. O. T. Karvinen, B. Jakobsson, and J. Randrup, Nucl. Phys. **A333**, 285 (1980).

¹⁴M. C. Robel, Lawrence Berkeley Laboratory Report LBL 8181, 1979.

¹⁵S. Leray, G. La Rana, C. Ngô, M. Barranco, M. Pi, and X. Vinas, Z. Phys. A **320**, 383 (1985).

¹⁶W. Cassing and W. Nörenberg, Nucl. Phys. **A431**, 558 (1984).

¹⁷P. Netter, L. Lassen, R. Schreck, and H. Gemmeke, Nucl. Instrum. Methods **185**, 165 (1981).

¹⁸R. D. Amado and R. M. Woloshyn, Phys. Rev. Lett. **36**, 1435 (1976).

¹⁹M. Lifshitz and P. Singer, Phys. Rev. C **22**, 2135 (1980).

²⁰W. Bohne, W. Galster, K. Grabisch, and H. Morgenstern, Nucl. Instrum. Methods **A240**, 145 (1985).

²¹D. Hilscher, E. Holub, G. Ingold, U. Jahnke, H. Orf, H. Rossner, W. U. Schröder, H. Gemmeke, K. Keller, L. Lassen, and W. Lücking, in *Proceedings of the Workshop on Coincidence Particle Emission from Continuum States in Nuclei, Bad Honnef, 1984*, edited by H. Machner and P. Jahn (World-Scientific, Singapore, 1984), p. 268.

²²D. Hilscher, J. R. Birkelund, A. D. Hoover, W. U. Schröder, W. W. Wilcke, J. R. Huizenga, A. C. Mignerey, K. L. Wolf, H. F. Breuer, and V. E. Viola, Jr., Phys. Rev. C **20**, 576 (1979).

²³D. Hilscher, E. Holub, U. Jahnke, H. Orf, and H. Rossner, *Dynamics of Heavy-Ion Collisions, Proceedings of the 3rd Adriatic Europhysics Study Conference, Hvar, Yugoslavia, 1981*, edited by N. Cindro, R. A. Ricci, and W. Greiner (North-Holland, Amsterdam, 1981), p. 225.

²⁴J. Gosset, H. H. Gutbrod, W. G. Meyer, A. M. Poskanzer, A. Sandoval, R. Stock, and G. D. Westfall, Phys. Rev. C **16**, 629 (1977).

²⁵W. Cassing, in *Proceedings of the Workshop on Coincidence Particle Emission from Continuum States in Nuclei, Bad Honnef, 1984*, edited by H. Machner and P. Jahn (World-Scientific, Singapore, 1984), p. 340.

²⁶K. Geoffroy Young, D. G. Sarantites, J. R. Beene, M. L. Halbert, D. C. Hensley, R. A. Dayras, and J. H. Barker, Phys. Rev. C **23**, 2479 (1981).

²⁷W. U. Schröder and J. R. Huizenga, in *Treatise on Heavy-Ion Science*, edited by D. A. Bromley (Plenum, New York, 1984), Vol. 2.

²⁸E. Holub, M. Korolija, and N. Cindro, Z. Phys. A **314**, 347 (1983).

²⁹M. Blann, Phys. Rev. C **31**, 1245 (1985).

³⁰J. J. Griffin, Phys. Rev. Lett. **17**, 478 (1966).

³¹N. Cindro, M. Korolija, and E. Holub, in *Fundamental Problems in Heavy-Ion Collisions, Proceedings of the Fifth Adriatic International Conference on Nuclear Physics*, edited by N.

Cindro, W. Greiner, and R. Čaplar (World-Scientific, Singapore, 1985), p. 301.

³²H. Machner, Z. Phys. A **321**, 577 (1985).

³³H. Machner, Z. Phys. A **302**, 125 (1981).